Electronic Supplementary Material (ESI) for Energy & Environmental Science.

Supporting Information

Boosting Water Decomposition by Sulfur Vacancy for Efficient CO_2 Photoreduction

Shikang Yin[a], Xiaoxue Zhao[a], Enhui Jiang[a], Yan Yan[a,*], Peng Zhou[b,*], Pengwei Huo[a,*]

[a]*Institute of Green Chemistry and Chemical Technology, School of Chemistry and Chemical Engineering, Jiangsu University, Zhenjiang 212013, PR China,*

[b]*Department of Electrical Engineering and Computer Science, University of Michigan, Ann Arbor, MI 48109，USA.*

Supplementary Methods

Materials

Tin chloride pentahydrate ($SnCl_4•5H_2O$), L-cysteine ($C_3H_7NO_2$), sodium dodecyl benzenesulfonate (SDBS), ethanol (C_2H_5OH) and ethylene glycol ($C_2H_6O_2$) were all purchased from Sinopharm Chemical Reagent Co., Ltd. Heavy oxygen water (Saen Chemical Technology Co., Ltd., 99% atom purity). $^{13}CO_2$ (99%) gas was obtained from Sigma-Aldrich Company Ltd. All reagents used in the synthesis were analytically pure and had not been further purified.

Preparation of pristine SnS_2 atomic thin layer

Atomic-layered SnS_2 was synthesized through a modified protocol based on the report literature. In a typical synthetic procedure, $SnCl_4·5H_2O$ (0.25 mmol), L-cysteine (2.5 mmol) and SDBS (0.8 mmol) were dissolved in deionized water (25 mL), stirred for 20 min, forming a homogeneous solution. The resulting solution was then transferred to a 50 mL autoclave and kept in 160 °C for 12 h. When the autoclave was cooled to room temperature, the final product was collected, washed with deionized water and ethanol for several times, and then freeze-dried in vacuum for further uses.

Preparation of Vs-SnS_2

Vs-SnS_2 catalysts were prepared by bombarding the pristine SnS_2 atomic thin layer sample through Ar plasma sputtering. The pristine SnS_2 powder was first put into a quartz reactor and treated with dielectric barrier discharge plasma. After the reactor was evacuated, Ar gas was used as the reaction gas to maintain a certain flow rate. Plasma bombard was performed at room temperature with 100 W input power. Treated for 1 min, 3 min, 5min and 7 min, respectively, resulting samples were labeled as V_S-SnS_2 with different S-vacancy concentrations.

CO_2 Photoreduction experiments

CO_2 photoreduction was carried out in a sealed self-made 300 mL stainless-steel reactor with a 300 W Xenon lamp (1000 $mW·cm^{-2}$) as the white light source. In a typical procedure, 5 mg catalyst was dispersed in 5 ml of deionized water. The resulting mixture was dropped on quartz glass, and then dried at 60 °C. The dried catalyst was placed in the stainless-steel reactor with 2 mL H_2O. CO_2 was then introduced into the reactor for 20 min to completely remove air. During the reaction, Xenon lamp illuminated the catalyst sample through the quartz window (22.1 cm^2). Gas products were detected by a gas chromatography (GC-7920, China) equipped with hydrogen flame ionization detector (FID).

Characterizations

Crystalline structures of catalysts were examined on an X-ray diffraction machine (XRD model MAC Science, Japan). Elemental orbit information was investigated using X-ray photoelectron spectroscopy (XPS, PHI 5300, PerkinElmer). The scanning electron microscopy (SEM) images were characterized on a field emission scanning electron microscope (FE-SEM, JSM-7001F, Japan). High-resolution transmission electron microscopy (HRTEM), corresponding selected area electron diffraction (SAED) spectra, and scanning transmission electron microscopy with spherical aberration corrector (AC-STEM) were carried out on a JEM-2010 transmission electron microscope (Japan). The texture and thickness of samples were measured by atomic force microscopy (AFM, MFP-3D, America). The ultraviolet-visible diffuse reflectance spectroscopy (UV-vis DRS) was carried out on a Shimadzu UV-3600 spectrometer. The S-vacancy concentration of samples was quantified by the inductively coupled plasma optical emission spectrometry (ICP-OES, 720, Agilent).

In-situ DRIFTS experiments

In-situ diffuse reflection infrared Fourier transform spectroscopy (DRIFTS) experiments were conducted on a Nicolet iS10 (Thermo) machine. In a typical procedure, catalyst sample was sealed in the reaction chamber with a quartz window. CO_2 and H_2O were carried into the reaction chamber by N_2 flow until equilibrium. After taking the equilibrium system before reaction as the blank background, IR signals were collected *in-situ* during the incident irradiation of a 450 nm LED lamb (3W) through the quartz glass window.

Photo-electrochemical measurements

The corresponding electrode was prepared as follows: 0.03 g of the prepared photocatalyst was dispersed in 3.0 ml of ethanol and 0.03 ml of oleic acid, and then 0.01 g of polyvinylpyrrolidone (PVP) was added. The above mixture was spin-coated on a 1×1 cm^2 fluorine-doped tin oxide glass electrode, and then dried at room temperature. The measurement system includes a standard three-electrode quartz cells with 0.5 M Na_2SO_4 electrolyte solution, a Pt wire and a saturated calomel electrode (SCE) were used as the counter electrode and the reference electrodes, respectively. Electrochemical impedance spectroscopy was performed in a mixture solution (0.1 M potassium chloride, 0.005 M potassium ferricyanide and 0.005 M potassium ferrocyanide) with a frequency range from 0.1 Hz to 100 kHz at 0.5 V. The amplitude of applied sine wave potential in each case was 5 mV which was carried out using the Chen Hua electrochemical workstation, and all electrochemical signals were recorded by a CHI660 B electrochemical analyzer (Chen Hua Instruments, Shanghai, China).

Computational Methods

The OER process of SnS_2 were investigated by the Vienna Ab-initio Simulation Package (VASP) with the revised Perdew-Burke-Ernzerhof (RPBE) of the generalized gradient approximation (GGA). PAW pseudo-potential was used to describe the interaction between ionic and valence electrons. A 3×4 {001} supercell containing one S-Sn-S layer was used to simulate SnS_2 surface. The cutoff energy of 1×10^{-4} eV and energy convergence of 400 eV were used in the geometry optimization. The S vacancy was built by removing one surface S atom. The reported standard hydrogen electrode (SHE) model (Nørskov J K, Rossmeisl J, Logadottir A, et al. Origin of the overpotential for oxygen reduction at a fuel-cell cathode. J Phys Chem B 2004; 108: 17886-17892) was adopted in the calculations of Gibbs free energy changes (ΔG) of all reaction steps, which was used to evaluate the reaction barrier. The chemical potential of a proton-electron pair, $\mu(H^+) + \mu(e^-)$, is equal to the half of the chemical potential of one gaseous hydrogen, $1/2\mu(H_2)$, at $U = 0$ V *vs* SHE at pH = 0.

Supplementary Figures

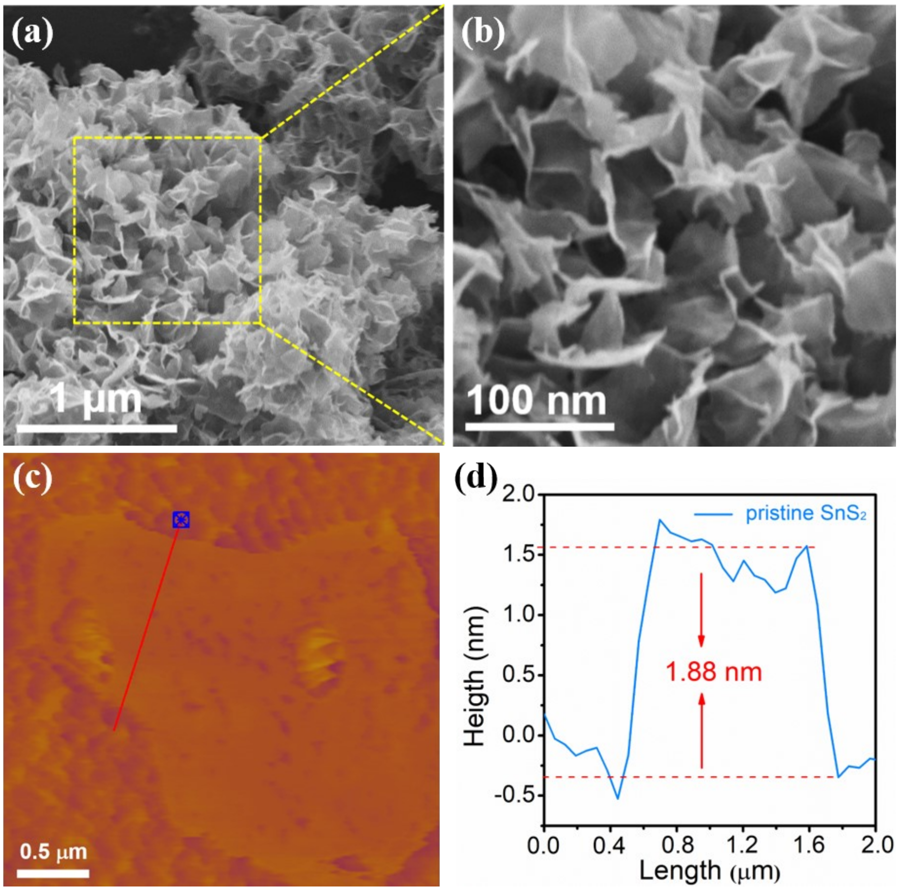

Figure S1. (a, b) SEM image of pristine SnS_2; (c, d) AFM image and the line-sweep profile for pristine SnS_2.

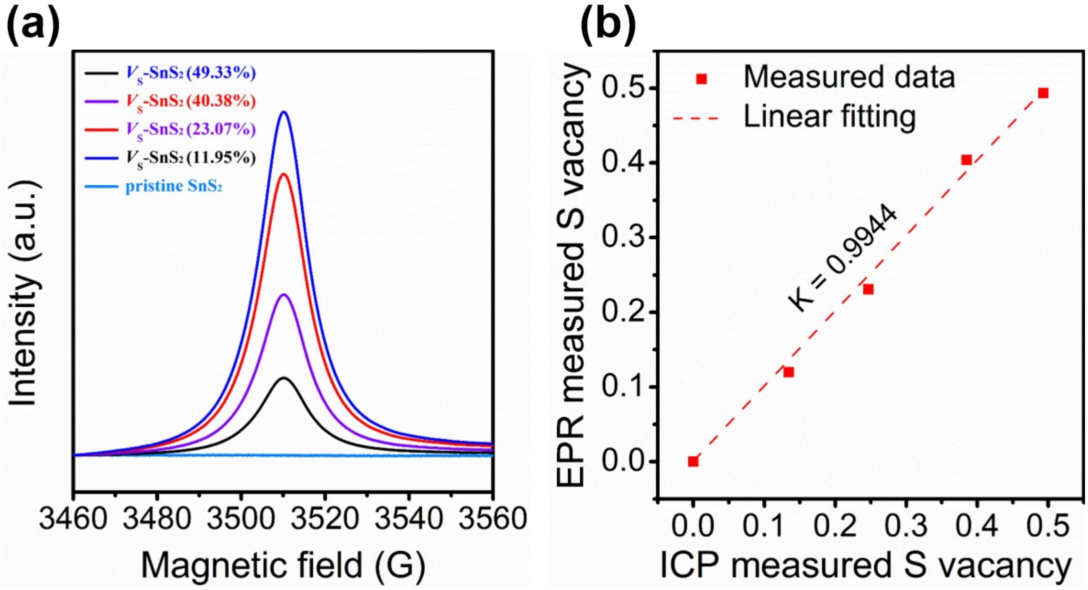

Figure S2. (a) The integrated EPR spectra of pristine SnS$_2$ and the V_S-SnS$_2$ with different S-vacancy concentrations; (b) the linear fitting between ICP quantified S-vacancy and EPR quantified S-vacancy according to Table S1.

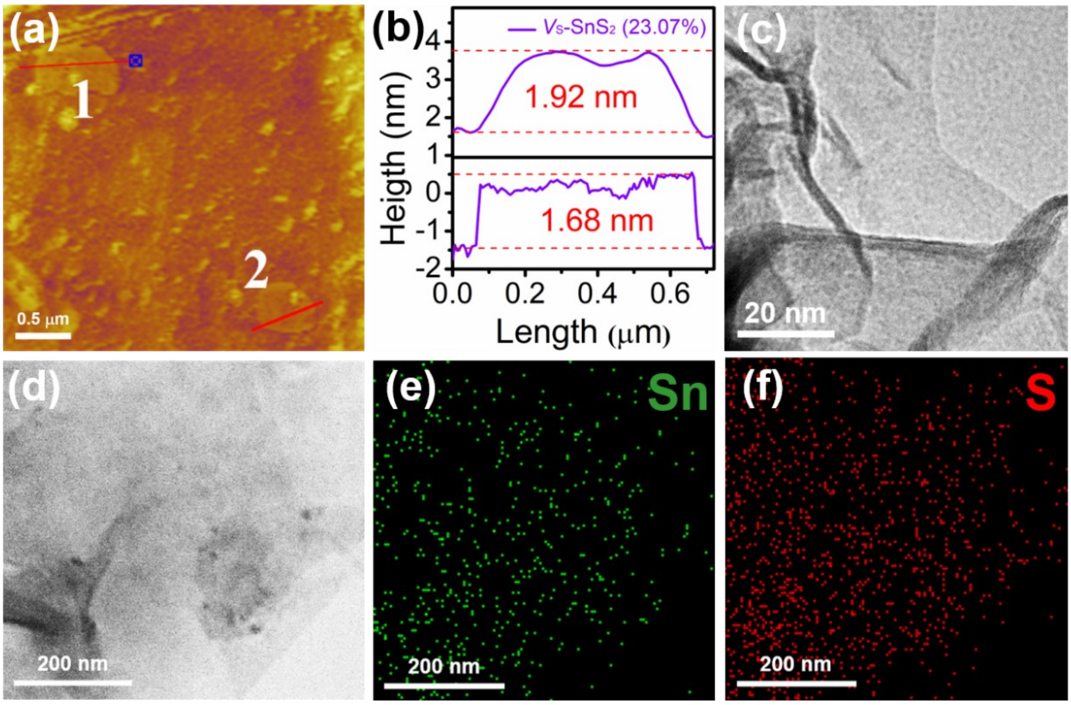

Figure S3. (a, b) AFM image and a thickness of between 1 nm and 2 nm for V_S-SnS$_2$ (23.07%), (c, d) TEM image of V_S-SnS$_2$ (23.07%); (e, f) corresponding Sn, S element mapping of V_S-SnS$_2$ (23.07%), respectively.

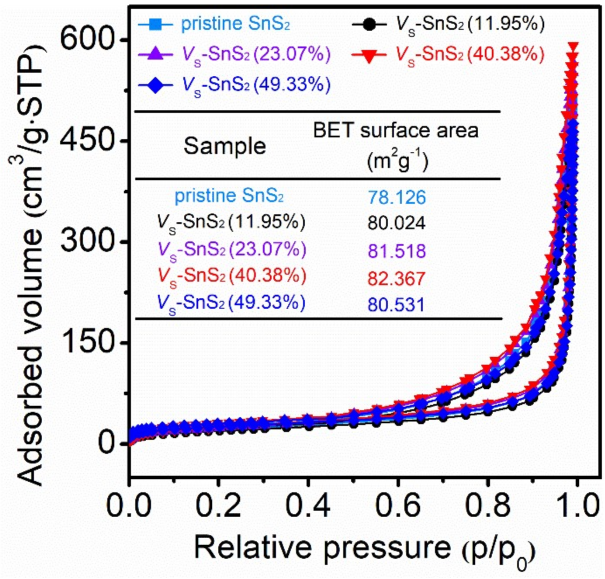

Sample	BET surface area (m^{2}g^{-1})
pristine SnS2	78.126
V_s-SnS2 (11.95%)	80.024
V_s-SnS2 (23.07%)	81.518
V_s-SnS2 (40.38%)	82.367
V_s-SnS2 (49.33%)	80.531

Figure S4. The N_2 adsorption-desorption isotherm measurements of the pristine SnS_2 and V_S-SnS_2 with different S-vacancy concentrations. Inset shows the BET surface area of different samples.

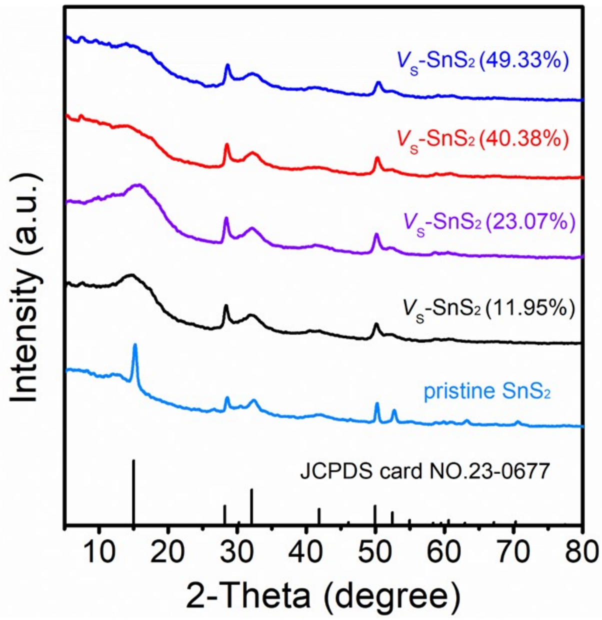

Figure S5. XRD patterns of the pristine SnS_2 and V_S-SnS_2 with different S-vacancy concentrations.

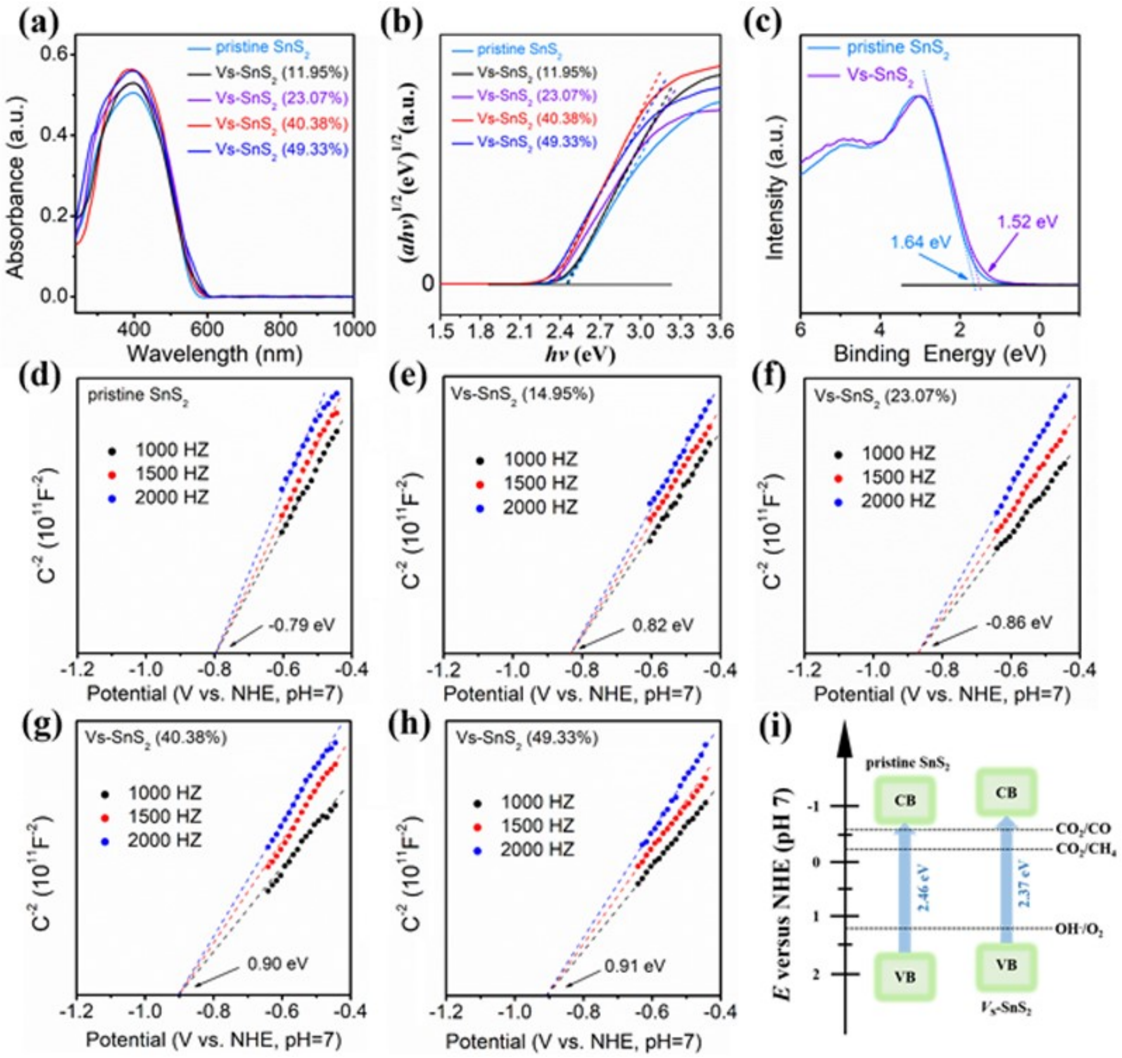

Fig. S6. (a, b) The UV-vis DRS spectrum and plots of $(ahv)^{1/2}$ versus of the pristine SnS_2 and different V_S-SnS_2 catalyst, respectively; (c) Valence band spectra of the pristine SnS_2 and V_S-SnS_2 (23.07%); (d, e, f, g, h) Mott-Schottky plots of the pristine SnS_2 and V_S-SnS_2 with different S-vacancy concentrations; (i) Band alignment of the pristine SnS_2 and V_S-SnS_2 (23.07%).

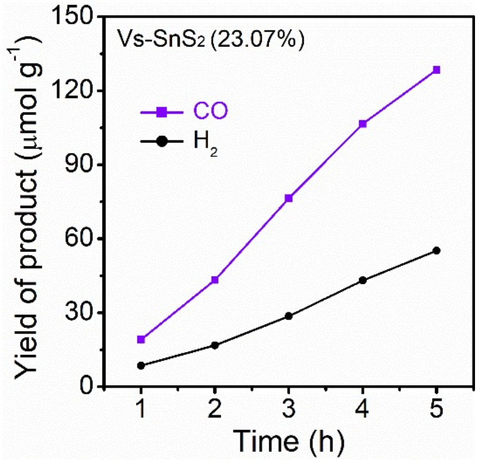

Fig. S7. The CO and H_2 evolution production for a complete reaction run in 5 hrs using the V_S-SnS_2 (23.07%).

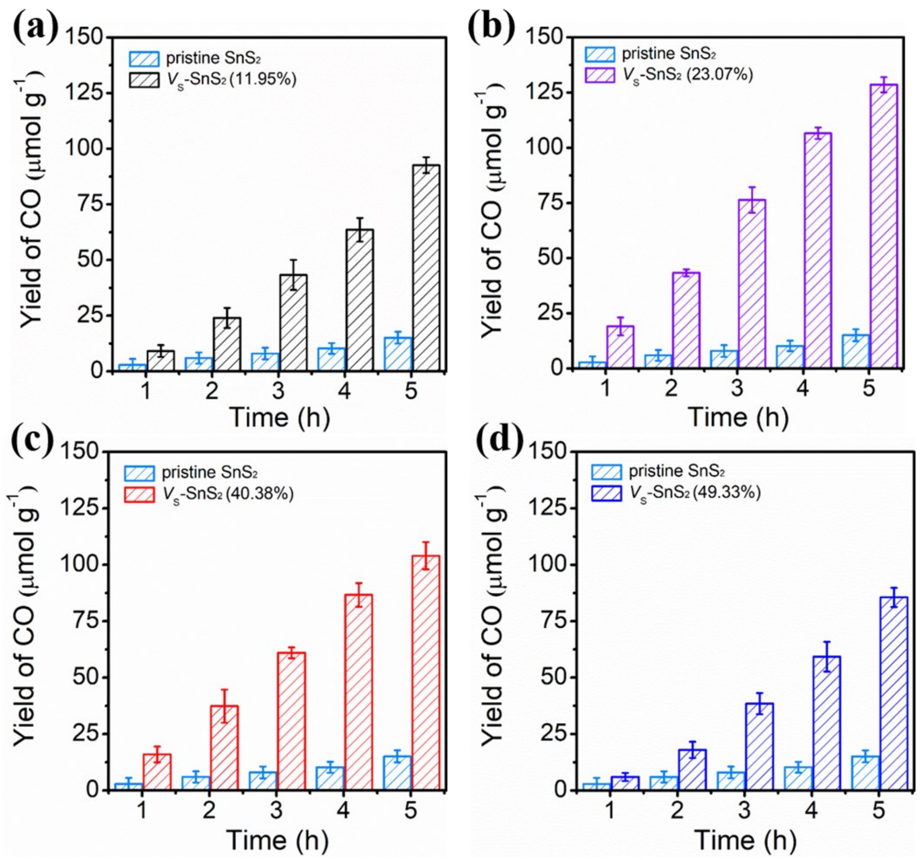

Figure S8. (a, b, c, d) Compared CO evolution performances of the pristine SnS_2 and V_S-SnS_2 with different S-vacancy concentrations, representing CO_2 photoreduction efficiencies. Error bar represents the standard deviation from three independent experiments.

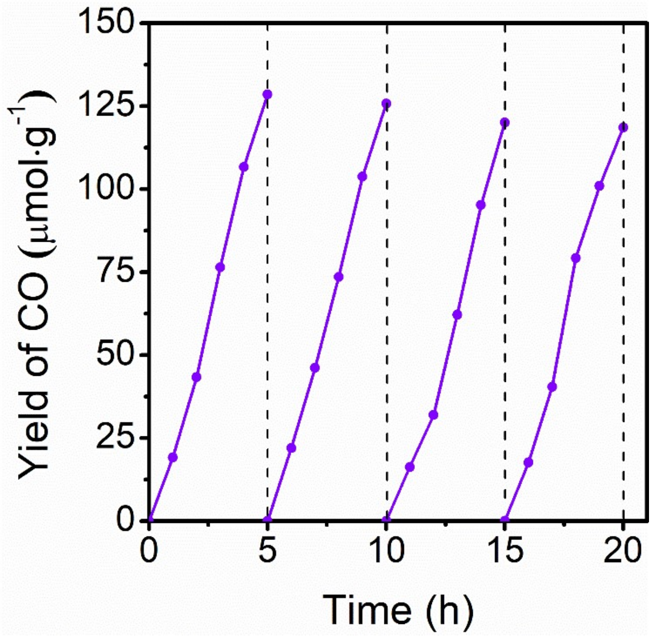

Figure S9. Cyclic CO evolution profiles of the champion V_S-SnS_2 (23.07%) catalyst in 20 hrs.

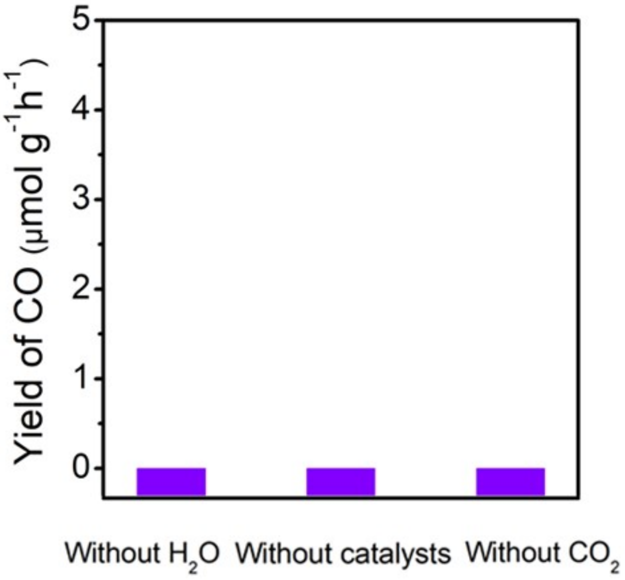

Figure S10. Control experiments in N_2 (without CO_2) or without photocatalysts or without H_2O for V_S-SnS_2 (23.07%) catalyst.

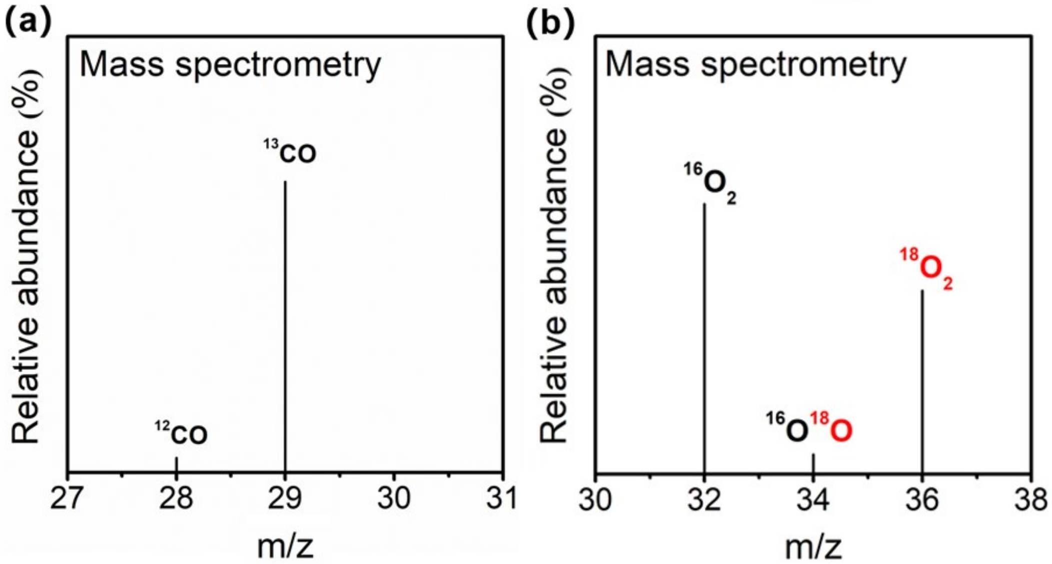

Figure S11. (a) Mass spectrum (m/z =29) analyses of ^{13}CO when relacing CO_2 with $^{13}CO_2$ in the overall CO_2 photoreduction on the champion V_S-SnS_2 (23.07%) catalyst. (b) Mass spectrum (m/z =36) analyses of $^{18}O_2$ when replacing H_2O with $H_2{}^{18}O$ in the overall CO_2 photoreduction on the champion V_S-SnS_2 (23.07%) catalyst.

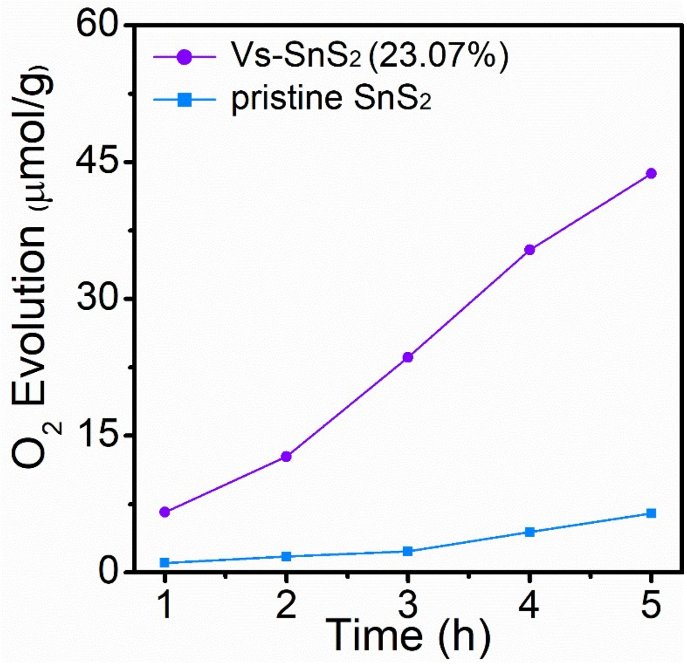

Figure S12. The comparison of O_2 production in overall CO_2 photoreduction on the pristine SnS_2 and V_S-SnS_2 (23.07%).

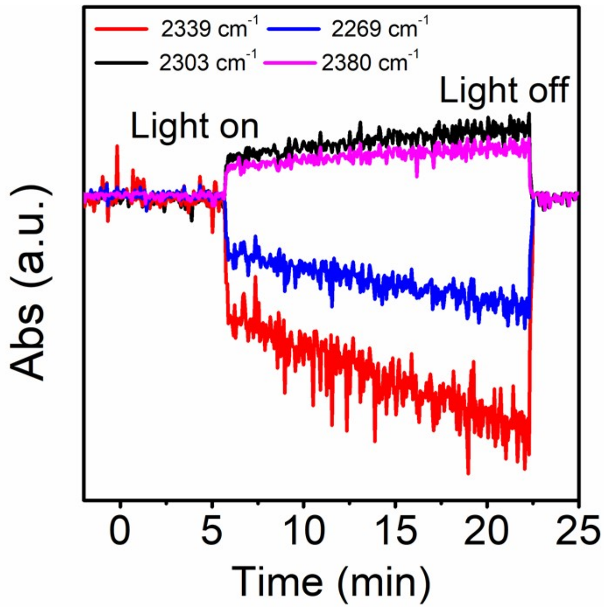

Figure S13. The kinetic profiles of 2339 cm^{-1} (red) and 2269 cm^{-1} (blue) correspond to 2303 cm^{-1} (black) and 2380 cm^{-1} (pink) from light-on to light-off, respectively, representing the reaction kinetics of CO_2 and corresponding intermediates.

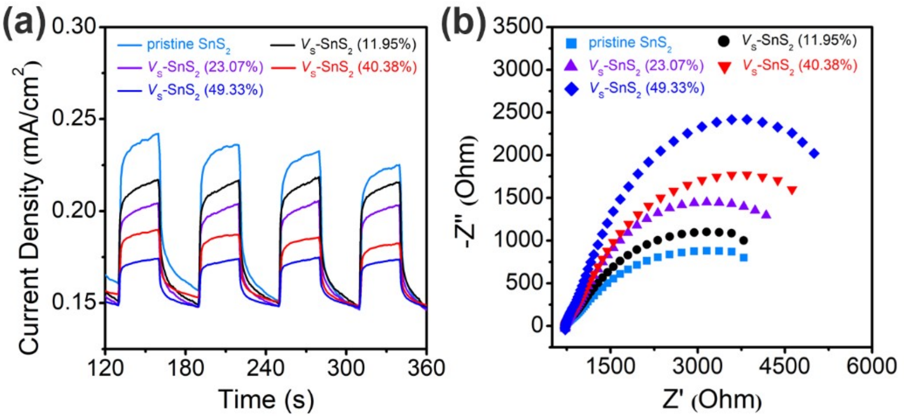

Figure S14. The photocurrent response of transient and electrochemical impedance spectroscopy for the pristine SnS$_2$ and *V*s-SnS$_2$ with different S-vacancy concentrations.

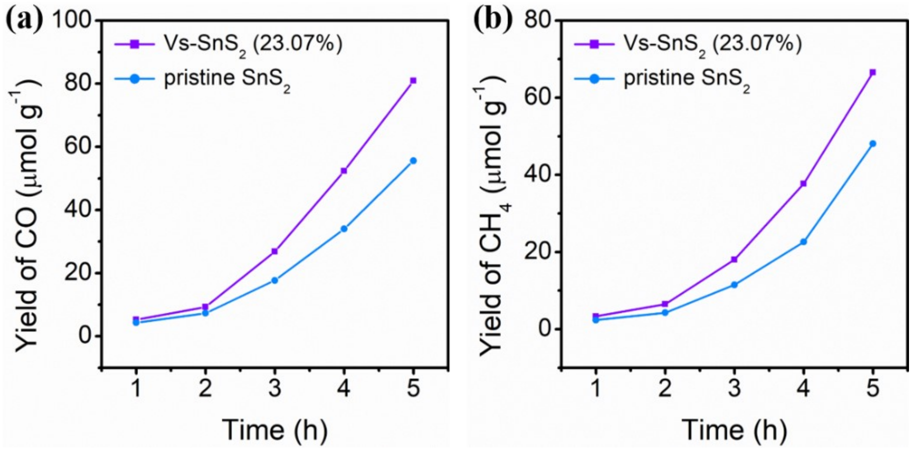

Fig. S15. (a, b) The comparion of CO and CH$_4$ evolution production for a complete reaction run in 5 hrs using the pristine SnS$_2$ and V_S-SnS$_2$ (23.07%), in which triethanolamine acts as a hole trap.

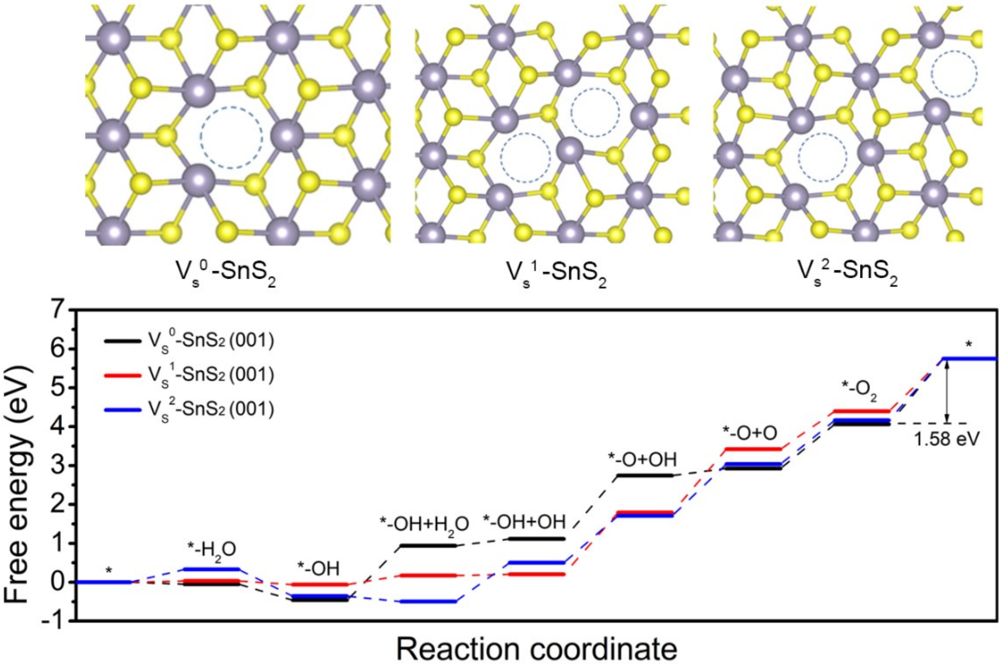

Figure S16. A 3×4 (001) supercell containing one S-Sn-S layer structural model for the V_S-SnS$_2$, the distance between two adjacent *V*s sites in V_S^0-SnS$_2$, V_S^1-SnS$_2$ and V_S^2-SnS$_2$ are 9.40 Å, 3.14 Å and 6.27 Å, respectively (the dashed circle indexes the removed S atom position); Gibbs free energy maps of the OER process simulated on the surface of the V_S-SnS$_2$ with different *V*s sites distance (where * represents the intermediate state).

Supplementary Tables

Table S1. ICP-OES characterization of pristine SnS_2 and the V_S-SnS_2.

Sample	Plasma treatment time (min)	ICP measured	EPR quantitative	S/Sn atomic ratio	BET surface area	Band gap (Kubelka-Munk function)
pristine SnS_2	0	0	0.01235	2.00	78.126	2.46
Vs-SnS_2	1	0.13452	0.11951	1.82	80.024	2.44
	3	0.24674	0.23073	1.57	81.518	2.37
	5	0.38522	0.40384	1.33	82.367	2.35
	7	0.49326	0.49326	1.17	80.531	2.32

EPR quantification data was obtained by the ICP characterization data proportional to the integrated absolute peak area of EPR spectra.

Table S2. AQEs of photoreduction CO_2 over V_S-SnS_2 under different wavelengths.

Wavelength (nm)	400	420	450	500	550
CO evolution (μmol)	0.108	0.598	2.278	1.427	0.124
Light intensity ($mW \cdot cm^{-2}$)	6.34	3.06	8.70	9.54	11.02
Irradiation area (cm^2)	22.1	22.1	22.1	22.1	22.1
Irradiation time (h)	5	5	5	5	5
AQE (%)	0.013	0.028	0.035	0.018	0.007

Reaction condition: 1 mg/ml V_S-SnS_2 solution dropwise to the quartz glass, and dry in an oven at 60 °C, 2 mL distilled water. All reaction was carried out at room temperature.

When λ=400 nm：

The number of incident photons:

$$N = \frac{E\lambda}{hc} = \frac{6.34 \times 22.1 \times 10^{-3} \times 5 \times 3600 \times 400 \times 10^{-9}}{6.626 \times 10^{-34} \times 3 \times 10^{8}} = 5.05 \times 10^{21}$$

AQE:

$$AQE = \frac{2 \times the\ number\ of\ evolved\ CO\ molecules}{N} \times 100\% = \frac{2 \times 6.02 \times 10^{23} \times}{5.05 \times} = 0.013\%$$